FORCED WAVES PROPAGATION IN GREAT LIVING ARTERIES TISSUES

ISABELLA BARBIERI

Department of Mathematics
University of Bologna
P.zza di Porta S. Donato 5, Bologna 40126, Italy
isabella.barbieri@unibo.it

EZIO CAROLI*

INAF/OAS di Bologna
Via Gobetti 101, Bologna 40129, Italy
caroli@iasfbo.inaf.it

GIOVANNI PALLOTTI

Department of Physics and Astronomy
University of Bologna
Via Berti Pichat 6/2, Bologna 40127, Italy
giovanni.pallotti@unibo.it

Received 5 May 2017
Accepted 1 March 2018
Published 10 May 2018

Starting from experimental data, this work exploit the similarity of pressure and axial wave's propagation of both pressure and axial waves in large vessel (e.g., aorta) with the solution of a mathematical model developed to describe the motion of acoustic waves in solid. In particular, we show how the motion parameters derived by fitting the experimental data measured in living dog arteries are related to mechanical properties of the vessel tissue using the same theoretical model. Furthermore, we briefly discuss the consequence on the predicted forced wave motion of inferring from experimental data a phase velocity depending from frequency.

Keywords: Wave propagation; great arteries; pressure wave; axial wave; phase velocity; amplitude attenuation; forced oscillations.

1. Introduction

The problem approached in the present work is a further development of the investigation of the tissues mechanical properties of the large vessels in the cardiovascular system. In particular, in the following section we will show how a mathematical model

*Corresponding author.

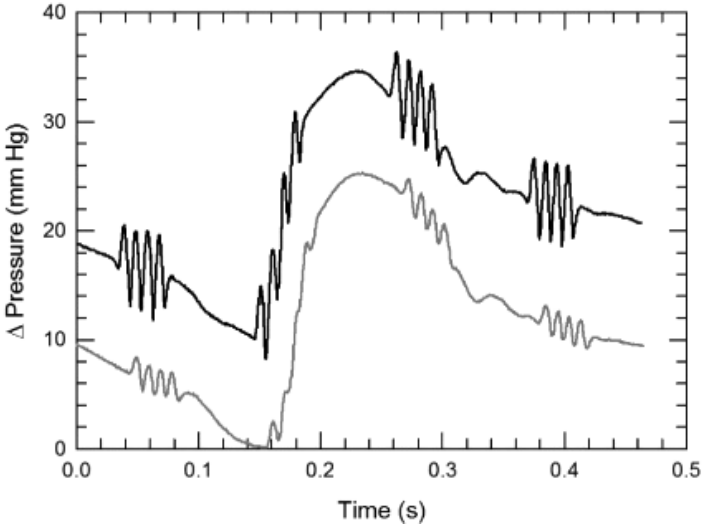

Fig. 1. Sinusoidal wave trains (100 Hz) super-imposed on the natural (sphygmic) pulse wave acting a as carrier. These curves are a sample of the ones measured by Anliker and collaborators in the experiment performed in vivo on dog carotid artery. The two plots show the pressure variation in time in two distinct section of the dog carotid: the grey line is measured 5 cm more distant.

developed to explain the motion of seismological wave propagation could explain experimental results obtained in living large arteries tissue.

Our research start from the experimental study and the subsequent theoretical justification of the results obtained by M. Anliker and collaborators on the transmission of axial, pressure and torsion forced waves in the large vessels of wolf dogs.[1] Figure 1 shows a sample of the wave propagation measurement obtained by Anliker *et al.* with its apparatus during the experiment, in which is clearly visible the stimulated wave trains (at 100 Hz) superimposed to the sphygmic carrying wave. The graph shows also the attenuation effect of the stimulated wave amplitude along the dog carotid artery at a given distance (5 cm).

These animals were used owing the great similarity of their large vessels with the man ones and because the measurements were possible to be made on living tissues of living bodies.

Further motivation for our data selection belong to compared medicine and we have preferred to perform our work starting from Anliker's results instead to consider other data obtained during autopsies, because these samples present a large variability due to the quite different variety of both pathological and test preparation conditions.

2. Experimental Results Summary

The results obtained by Anliker's group in their "*in vivo*" experiment on large vessels,[2] are summarized in Fig. 2 that shows, respectively, the velocities and the

attenuation measured for two induced mechanical waves types: along the axis (y direction) of the vessel (axial) and transversal (i.e., orthogonal) to the same axis (pressure) oscillations.

The behavior (Fig. 2) of the results of Anliker's work on wave transmission along arteries give in particular two fundamental results: the wave propagation velocity is

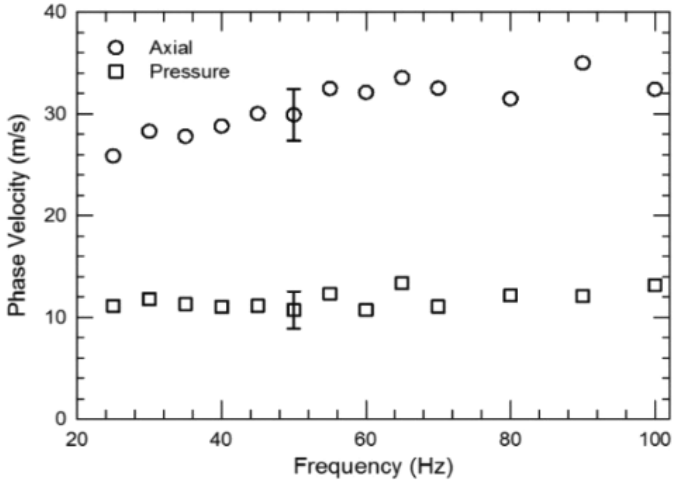

(a)

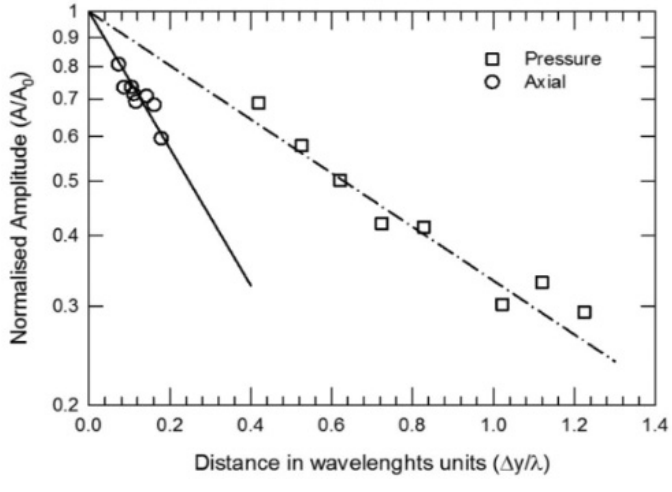

(b)

Fig. 2. Summary of Anliker experiment results for axial and pressure forced wave. (a) Phase velocity as function of forced wave frequency. The error bar superimposed to one point of each data set represents the 1σ average experimental error over the entire measurements sample. (b) Wave amplitude attenuation as function of distance in wavelength units. Each data point represents the average of six independent experiments.

essentially constant (i.e., independent from the wave frequency) and the wave amplitude is attenuated exponentially with distance.

Using a chi-square test, we confirmed that the Phase velocity data measured in the "*in vivo*" experiment are compatible with constant values. In fact, we obtain a confidence greater than 95% for the case of pressure waves, while for axial ones the statistical confidence is slightly less than 90%. Indeed, in the case of axial waves the experimental data in Fig. 2(a) show a weak frequency dependence that in first instance can be considered within the experimental errors. In particular, the measured average phase velocities are $11.7 \pm 0.2\,\mathrm{m/s}$ and $30.8 \pm 0.7\,\mathrm{m/s}$ for pressure and axial waves respectively.

In Fig. 2(b), the attenuation of the two wave types is reported, showing that the amplitude exponential attenuation is function of the forced oscillation wavelength for both types of mechanical waves and of the distance from the origin along the vessel. A simple exponential function fits the two experimental data sets:

$$A/A_0 = e^{-\alpha\frac{\Delta y}{\lambda}}, \tag{1}$$

where A/A_0 is the normalized amplitude, α represent the dimensionless attenuation factor, Δy is the distance along the vessel from the forced oscillation application point and λ is the wavelength. The fit gives a value of 1.1 and 3.6 for the attenuation constant of pressure and axial wave respectively, with a significance of $\sim$90%.

The meaning of the last Anliker's results is that the attenuation of the forced wave amplitude is the same for each frequency. Therefore, the amplitude of each forced oscillation decrease of the same quantity for the same number of wavelength from the origin. For example, the amplitude of a 20 Hz pressure (axial) wave decrease of a $1/e$ factor at 0.532 (0.42) m from origin, while at 100 Hz the same amplitude attenuation is measured at 0.106 (0.085) m. In both case, as well for all the frequencies, the distance in wavelength units has the same value of 0.91 (0.28).

3. Model and Theoretical Discussions

The characteristics of forced wave propagation described in the previous section, suggest that we can consider live large vessel tissue as a Knopoff body[3] and try to analyse the propagation of pressure and axial waves similarly to the propagation of acoustic wave in solid.

With this assumption for blood vessel tissue, the pressure wave (e.g., shear waves in Knopoff nomenclature) motion can be described by the following differential equation:

$$\rho\frac{\partial^2\bar{u}}{\partial t^2} = \mu_E\frac{\partial^2 u}{\partial y^2} + \mu_v\frac{\partial^3\bar{u}}{\partial t\partial y^2}, \tag{2}$$

where ρ is the density (g/cm^3), t is the time (s) and y the linear coordinate (parallel to the vessel axis), while μ_E and μ_v are the medium elastic and viscosity constant, respectively.

In Eq. (2), $u = u(t, y)$ represent the total displacement given by $\bar{u} = u_p + u$, where where u_p is the permanent (irreversible) displacement and u the recoverable displacement. Since the permanent displacement (i.e., deformation) is negligible with respect to the elastic deformation for low attenuation factor, in the wave motion equation we can use only the elastic displacement u.

Following Knopoff, Eq. (2) with the assumption of elastic displacement only can be rewritten as an equation that combines a linear term, corresponding to a Kelvin Voigt Maxwell solid, with a nonlinear term which takes into account the interaction between the two processes (elastic and viscous). If the loss due to each of these mechanisms separately can be considered small even the effect of their interaction of will be very small and therefore the nonlinear term can be simplified and the wave motion equation can be rewritten as:

$$\frac{\partial}{\partial y}\left[\frac{\partial^2 u}{\partial y^2} - \frac{1}{V_P^2}\frac{\partial^2 u}{\partial t^2} + \frac{\mu_v}{\mu_E}\frac{\partial^3 u}{\partial y^2 \partial t} - 2\mu_c \rho \frac{\partial u}{\partial t}\right] = 2\eta_c \rho \frac{\partial}{\partial t}\left[\left|\frac{\partial^2 u}{\partial y \partial t}\right| \mathrm{sgn}\left(\frac{\partial u}{\partial y}\right)\right], \tag{3}$$

where, in addition to already defined constants, μ_c is a constant having the dimension of inverse of viscosity, η_c represents the Columbian deformation impedance and finally V_P is the elastic pressure wave velocity:

$$V_p = \sqrt{\frac{\mu_E}{\rho}}. \tag{4}$$

In Eq. (3), the nonlinear term can be considered negligible in comparison with the elastic wave propagation term. Therefore, a quasi-harmonic solution can be obtained using the Krylov and Bogoliubov method assuming a solution of the form[4,5]:

$$u = A(t, y)\sin(ky - \omega t + \phi(t)). \tag{5}$$

If we assume that the amplitude function $A(t, y)$ can be decoupled in time and space as $A(t)B(y)$ and both $A(t)$ and the phase $\phi(t)$ are slowly variable in time we can obtain the following solution for the pressure elastic displacement:

$$u(t, y) = A_0 e^{-\left(\frac{\mu_v}{\mu_E}\frac{\omega^2}{2V_p} + \frac{2}{\pi}\eta_c \rho V_p \omega + \mu_c \rho V_p\right) y} \sin(ky - \omega t + \phi_0). \tag{6}$$

As discussed in Ref. 3, the zero and second power term in frequency results from linear dissipation terms in the wave equation (attenuation in Maxwell and Kelvin–Voigt solids). There are some condition (i.e ranges of frequency) for which both these terms in the wave attenuation coefficient are negligible with respect to the ω first order in the exponential argument. Equation (6) describe the behavior of pressure wave motion in the Anliker experiment if we assume that the frequency range of the forced induced waves satisfied the previous condition. In fact, neglecting both the ω^2 and the constant terms in the exponential factor, and considering that the phase velocity is constant with frequency ($V_P = \omega\lambda/2\pi$), Eq. (6)

can be simply rewritten, in term of wavelength as

$$u(t,y) = A_0 e^{-4\eta_c \rho V_P^2 \frac{y}{\lambda}} \sin(ky - \omega t + \phi_0) = A_0 e^{-\frac{\alpha_P y}{\lambda}} \sin(ky - \omega t + \phi_0), \tag{7}$$

where $\alpha_P = 4\eta_c \rho V_P$ is a constant that depend on the Columbian impedance of the vessel tissue and on its elastic coefficient that define the pressure wave velocity. In Eq. (7), A_0 is the wave amplitude and λ its wavelength.

Following the model developed by Knopoff, we can solve in a similar manner the equation of motion for the axial waves (i.e., longitudinal waves in Ref. 3). The solution given for this type of forced oscillation has the same form of Eq. (7), but with different tissue mechanical parameters involved:

$$u(t,y) = Ae^{-\left(\frac{\lambda_v + 2\mu_v}{\lambda_E + 2\mu_E} \frac{\omega^2}{2V_A} + \frac{4}{3\pi}\psi_c \rho V_A \omega + \frac{2}{3}\mu_c \rho V_A\right) y} \sin(ky - \omega t + \phi_0). \tag{8}$$

As before in a defined range of frequency, the exponential in the solution of motion become only linearly dependent from the wave radial frequency ω, and for a constant phase velocity we can rewrite also in this case the exponential term in Eq. (8) as function of the wavelength λ:

$$u(t,y) = A_0 e^{-\frac{8}{3}\psi_c \rho V_A^2 \frac{y}{\lambda}} \sin(ky - \omega t + \phi_0) = A_0 e^{-\frac{\alpha_A y}{\lambda}} \sin(ky - \omega t + \phi_0), \tag{9}$$

where ψ_c is a constant having the dimension of the invers of stress (m^2/N). As for the pressure wave case, the axial wave attenuation α_A depend on their phase velocity V_A that is defined by

$$V_A = \sqrt{\frac{\lambda_E + 2\mu_E}{\rho}}, \tag{10}$$

in which λ_E represent the volume compressibility and μ_E is the elastic coefficient of the vessel tissue.

Equations (4) and (10) for phase velocity are constant or slowly variable with frequency because of the physical parameters characteristics on which they depends. Therefore, the phase velocity expressions derived from the Knopoff model are consistent with the experimental results reported above. Furthermore, the two Eqs. (7) and (9) that represent the modification of the deformation for pressure and axial wave respectively exhibit exponential attenuation of the amplitude as function of the wave frequency. This, being the phase velocity constant, means that the amplitude attenuation depends on the oscillation wavelength as observed in the experimental data.

Using the phase velocities measured by Anliker in Eqs. (4) and (10), obtained by solving the motion equations for axial and pressure waves obtained using Knopoff *et al.* model, we can derive the values for the vessel wall elastic constant μ_E and volume compressibility λ_E. In particular, we obtain $\sim 1.51 \times 10^3\,\mathrm{N/m^2}$ and $\sim 6.63 \times 10^3\,\mathrm{N/m^2}$ respectively for these two material characteristics. These

numbers are compatible with known (or measurements obtained) values for living large vessel tissues and other evaluations.[6]

Using these values for the elastic parameters of vessel tissue in the exponential coefficient of Eqs. (7) and (8), and the estimates of the wave amplitude attenuation obtained in Anliker's measurements, we can obtain an evaluation of the coefficients η_c and ψ_c that represent the Columbian deformation impedance of the same tissue for pressure and axial waves, respectively:

$$4\eta_c \rho V_P^2 = \alpha_P; \quad \frac{8}{3} \; {}_c\rho V_A^2 = \alpha_A. \tag{11}$$

These two equalities with the values reported above for the different constants allow to obtain $1.83 \times 10^{-3}\,\mathrm{m}^2/\mathrm{N}$ for η_c and $4.66 \times 10^{-3}\,\mathrm{m}^2/\mathrm{N}$ for ψ_c, respectively.

Therefore, the use of the phase velocity and amplitude attenuation inferred by the Anliker's experimental data for forced waves in living dog great arteries in the simplified Knopoff model allow us to derive directly some parameters characterizing the mechanical properties of the living wall tissue. Table 1 report a summary of the evaluated values for both pressure and axial waves mechanical parameters.

As we already stated above, the adopted model is valid only in a limited wave frequency range. In fact, the solution of the pressure wave propagation model become of the form expressed in Eq. (7) only if the frequency of the travelling wave falls within a range defined by

$$\frac{\pi}{2}\frac{\mu_c}{\eta_c} \ll \omega = 2\pi\nu \ll \frac{4}{\pi}\frac{\eta_c \mu_E^2}{\mu_\upsilon}. \tag{12}$$

While for the case of forced axial wave propagation, the solution can be expressed by Eq. (9), if their frequencies are within the limits expressed by the following relation:

$$\frac{\pi}{2}\frac{\mu_c}{{}_c} \ll \omega = 2\pi\nu \ll \frac{8}{3\pi} \; {}_c\frac{(\lambda_E + 2\mu_E)^2}{\lambda_\upsilon + 2\mu_\upsilon}. \tag{13}$$

Both the inequalities defined in Eqs. (12) and (13) depend also on other mechanical parameters, such as λ_υ and μ_υ that are viscosities ($\mathrm{N/m^2}$) and μ_c, is a parameter characterizing Maxwell solid viscosity with the dimension on the inverse of viscosity ($\mathrm{m^2/N}$).

Table 1. Mechanical characteristics of living large vessel tissues directly evaluated from Anliker's measurements.

μ_E	$1.51 \times 10^3\,\mathrm{N/m^2}$	η_c	$1.83 \times 10^{-3}\,\mathrm{m^2/N}$
λ_E	$6.63 \times 10^3\,\mathrm{N/m^2}$	${}_c$	$4.66 \times 10^{-3}\,\mathrm{m^2/N}$

Substituting the values reported in Table 1 in Eqs. (12) and (13), these frequency constraints become, respectively for pressure and axial waves, the followings:

$$136.6\mu_c \ll \nu \ll \frac{845.5}{\mu_v}; \quad 53.65\mu_c \ll \nu \ll \frac{58381.8}{\lambda_v + 2\mu_v}. \tag{14}$$

To validate the Knopoff model used to explain the results obtained by Anliker and collaborators, we need to verify that the frequency limits, defined by the above expressions, include the range used for the experimental measurements for values of μ_v, λ_v, and μ_c compatible with the corresponding mechanical properties of biological tissues.

With respect to the reported experiments, we can assume that 1 Hz (1/20 of the minimum used frequency) can be considered low enough to satisfy the left limit of the frequency range. Therefore, we can immediately estimate the maximum values for μ_c able to satisfy simultaneously the lower constraints for both pressure and axial waves: $\mu_{cMax} \sim 7 \times 10^{-3}$ (m^2/N).

If we consider now the upper frequency limit, we can use the case of pressure wave to obtain an upper limit for the constant μ_v. Considering as high frequency limit a value ten time larger than the maximum frequency used in the Anliker's experiments (i.e., 100 Hz) we obtain $\mu_{vMax} \sim 0.85$ (N/m^2). Of course, this estimate for the maximum value of μ_v bounds, through the right term of Eq. (14), the range of values that the λ_v parameter can assume in the model. Using 1000 Hz as limiting frequency, the constant λ_v should range between 0 and ∼56.5 (N/m^2) to guarantee that the solution of the axial wave propagation have the form of Eq. (9), i.e., it is in agreement with the experimental results.

4. Forced Axial Wave Propagation with Phase Velocity Dependent on Frequency

As already pointed out, from the experimental data reported in Fig. 2(a) and as demonstrated by the chi-square constant test for the two types of forced oscillations, the assumption that the phase velocity of axial forced waves is constant with frequency is weaker than for pressure waves.

In fact, the behavior of axial phase velocity as function its frequency can be better described with a function presenting a dependence that tend to saturate with increasing frequencies. The phase velocity increase of ∼30% from 20 to 60–80 Hz and is almost constant in average (∼33 m/s) after 70 Hz. Following these indications, we tried to fit the axial wave data with different two parameters models exhibiting a saturation for increasing frequencies. The models, we used, are reported in Table 2, while Fig. 3 shows the best-fit results obtained with chosen functions superimposed to the original Anliker's experimental data for phase velocity of forced axial waves.

Both the adopted models depend on two parameters which an evident physical meaning: V_S represents the phase velocity at saturation (i.e., at high frequency), while ν_c is a characteristic frequency. The model based on a hyperbolic functions

Table 2. Models used to fit the axial waves phase velocity data and estimated parameters values. R represent the Regression correlation coefficient, while W is the Wilkinson test statistics.

Model 1	Exponential with saturation	$V_A(\nu) = V_S\left(1 - e^{-\frac{\nu}{\nu_c}}\right)$	$V_S = 33.2 \pm 0.6$ (m/s) $\nu_c = 17.5 \pm 0.2$ (Hz) $R = 0.91, W = 0.938$
Model 2	Hyperbolic	$V_A(\nu) = \frac{V_S \cdot \nu}{\nu_c + \nu}$	$V_S = 33.6 \pm 1.2$ (m/s) $\nu_c = 11.1 \pm 1.9$ (Hz) $R = 0.92, W = 0.947$

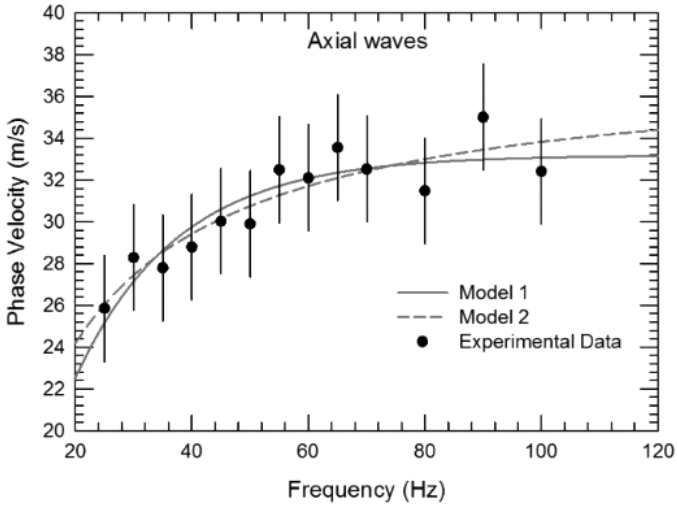

Fig. 3. Best-fit models (lines) over plotted to the Anliker's experimental data (filled circles) for the case of forced axial waves in the frequency range between 20 and 120 Hz.

follow better the phase velocity data behavior at low frequency (<50 Hz), while the exponential function are more compliant with data for high frequency (>50 Hz), and in particular this model exhibit a faster saturation as it seems indicated by data itself.

We should point out that even in the case of phase velocity depending on forced wave frequency does not change the model of the propagation and the wave motion solutions represented by Eqs. (8) and (9). The difference is that for a phase velocity depending on frequency we have a solution of the same form, but a different attenuation coefficient for each frequency. In particular, assuming the *Model* 1 for V_A, we can rewrite Eq. (9) in the following form:

$$u(t,y) = A_0 e^{-\frac{8}{3}\psi_c \rho V_S^2 (1-e^{-\omega/\omega_c})^2 \frac{y}{\lambda}} \sin(ky - \omega t + \phi_0) = A_0 e^{-\frac{\alpha_A y}{\lambda}} \sin(ky - \omega t + \phi_0), \quad (15)$$

where we have used the relation $\omega = 2\pi\nu$ in the phase velocity expression. The exponential factor in Eq. (15) has still the form of the Anliker's forced wave

attenuation, but with the amplitude attenuation coefficient depending from the frequency. Using the *Model* 1 in the range of frequency used in its experiments, the phase velocity change between 25.2 m/s at 25 Hz, and 33.1 m/s at 100 Hz. This implies a change in the amplitude attenuation coefficient. We assume that the axial wave attenuation coefficient of 3.6 measured by Anliker is the value for an "average" frequency in the 25–100 Hz range. Taking into account that the frequency dependence of the attenuation coefficient is exponential, we can evaluate such "*average*" frequency using the geometrical mean: $\overline{\omega} = \sqrt{25 \cdot 100} = 50$ Hz. For this frequency, the phase velocity is 31.3 m/s that is fully compliant with the constant value for axial wave evaluated by Anliker and collaborators (30.7 ± 0.7 m/s). Therefore, the attenuation coefficient at each frequency can be estimated using the following relationship:

$$\alpha(\nu) = 3.6\left(\frac{1 - e^{-\nu/\nu_c}}{1 - e^{-50/\nu_c}}\right)^2. \tag{16}$$

In the measured frequency range, the attenuation coefficient will then varies from ∼2.63 (at 25 Hz) to the 4.03 at 100 Hz. As expected, the impact of the inferred dependence of axial wave phase velocity on amplitude attenuation is greater at low frequency, for which the amplitude attenuation is significantly lower, 73% of the measured value with the assumption of a constant phase velocity.

Figure 4 shows the difference between the two attenuation cases over a frequency range much wider than the one used in the "*in vivo*" measurements by Anliker and collaborators, which lower limit is represented by the vertical grey line at 25 Hz.

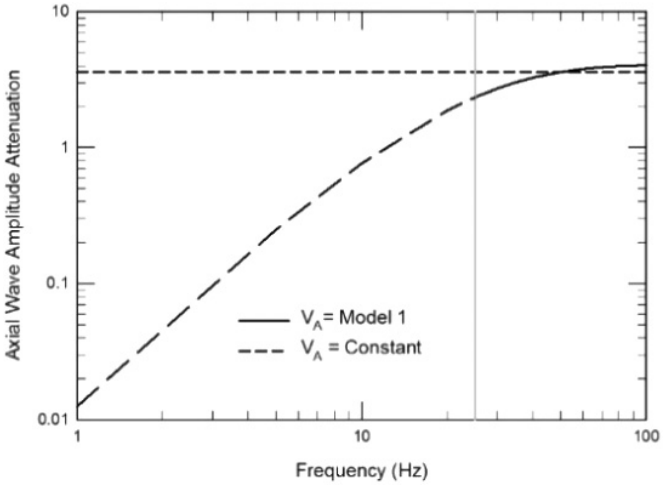

Fig. 4. The axial wave amplitude attenuation as function of frequency obtained by the phase velocity *Model* 1 (solid line) compared with the constant value of 3.6 (short dashed line) inferred by the experimental results assuming a constant phase velocity. The vertical grey line represent the lower frequency (25 Hz) used in the Anliker's measurements. The long-dashed line represents the extrapolation below this frequency for attenuation coefficient obtained using *Model* 1 for the axial wave phase velocity.

We made this extrapolation to point out that for an axial waves phase velocity depending from frequency as described by *Model* 1, the correspondent amplitude attenuation would strongly decrease as the frequency decrease. This behavior will therefore be more favorable for propagation of low frequency axial waves along great arteries tissues. In particular, for forced oscillation with basic harmonics around few Hz, such as the sphygmic wave, the expected attenuation is very low (0.015–0.05) allowing low amplitude attenuation over a long path: e.g., at 5 Hz, $1/e$ amplitude attenuation is expected in 6.6 m, and at 1 Hz in more than 100 m.

Figure 1, where the forced wave packets in two different positions along the dog aorta are super-imposed on the sphygmic pulse, qualitatively confirm the previous expectations. Finally, we should point out that expected behavior is equivalent to state that for very low frequency the tissues is almost perfectly elastics because the attenuation is negligible for typical lengths of large vessels in non-pathological conditions.[7]

5. Conclusion

We have shown that the propagation of forced oscillation in large vessel living tissues can be described with a model directly derived from the one used by Knopoff for earthquake induced oscillation in quasi elastic solid. The model give solution that are consistent with experimental data obtained "*in vivo*" conditions on dog carotids. In fact, the Knopoff model is able to give for the propagation of forced oscillation a behavior that have the same characteristics of ones measured by Anliker and collaborators, in terms of both attenuation of the waves amplitude with distance and phase velocity with frequency.

The results obtained from Anliker and collaborators for the propagation of the axial waves, which have a much greater attenuation (> 3 times) compared to those of pressure ones for wavelength unit length, suggest a variation of the phase velocity statistically significant, still compatible with the evaluated average value. Using a best-fit model with phase velocity saturating for increasing frequency, we have shown that the attenuation expected at very low frequencies, such as those of the basic harmonics of the sphygmic pulse, the attenuation becomes insignificant and the tissue of the arteries walls can be considered practically purely elastic.

Because our final target is to find a simple model able to explain the shape of the sphygmic wave generated by heart, we would prosecute on this direction trying to describe in next works the propagation of a finite wave packet along great arteries with almost pure elastic properties, but considering different impedance due to the overall systemic circulation.

References

1. Anliker M, Private communication (1969).
2. Moritz WE, Anliker M, Wave transmission characteristics and anisotropy of canine carotid arteries, *J Biomech* **7**:151–154, 1974.

3. Knopoff L, MacDonald JF, Attenuation of small amplitude stress waves in solids, *Rev Mod Phys* **30**:1178–1192, 1958.
4. Minorsky N, *Introduction to Non Linear Mechanics*, Edwards Brothers, Inc., Ann Arbor, pp. 186 and seq. (1947).
5. Krylov NM, Bogolyubov NN, *Introduction to Non-Linear Mechanics*, Princeton University Press, ISBN 9780691079851 (1947).
6. Pallotti C, Pallotti G, Roveri N, Some consideration on the mechanical properties of large vessels, *Biomechanics* **11**:19–25, 1981.
7. Newman DL, Greenwald SE, Denver HT, Impulse propagation in normal and stenosis vessel, *Cardiovasc Res* **15**:190–195, 1981.